I. Troch, F. Breitenecker, eds.      ISBN 978-3-901608-35-3

# UNSTEADY FLUID MECHANICS EFFECTS IN Water BASED LOCOMOTION

Peter Dabnichki Queen Mary University of London, London, UK

Corresponding Author: Peter Dabnichki, Queen Mary University of London, School of Engineering and Material Science, Mile End, Road, E1 4NS, London, UK, p.dabnichki@qmul.ac.uk

**Abstract**. Computational fluid mechanics (CFD) has made substantial progress on modelling a variety of important problems in industry. However, there is still lack of reliable methods to model the motion of the body in water. This is a central issue in understanding animal and human propulsion in water. The presented work demonstrates that a successful strategy is to model the unsteady effects and simultaneously utilise experimental data. This allows to simplify the resulting equations – potential flow vs turbulent flow. The use of boundary element method (BEM) proved very successful as it allowed to reduce this dynamic problem to a quasi-static one. The comparison between the experimental data and the simulation result was in the range of 95% suggesting that the added mass effect and dynamic lift and drag are the most significant physical phenomena in propulsive force generation.

## 1 Introduction

Water based locomotion as well as the flights of birds have been studied with a different intensity over the last 70 years. Most of the emphasis has been on development of analytical methods for estimation of the forces. However, such models have limited success as the resulting mathematical equations are too complex and analytical approximations are only appropriate for Stokes flow. The emergence of powerful Computational Fluid Dynamics (CFD) commercial packages shifted the attention towards the development of powerful computational methods that leads sometimes to compromise of physical models and mathematical rigour [2]. For example some of the most used computational methods such as Large Eddy Simulation (LES) and Direct Numerical Simulations are not proven mathematically but are very widely used in industry. However, there are still considerable gaps in our knowledge of the forces acting on accelerating bodies in water in general and the understanding of human and animal propulsion that utilise these effects [1,4,8,10]. Understanding of these effects has an important practical dimension – the use of these effects in biomimetic designs [7]. The author aimed to establish the physical soundness of the use of simpler but rigorous mathematical to model and assess the relative importance of different unsteady flow factors in modelling human arm propulsion during a front crawl stroke.

## 2 Modelling of the propulsion force

Research of human front crawl stroke has been conducted for more than 30 years as the main interest was the magnitude and time profile of the propulsive forces of the arm which is by far the greatest contributor. However, despite the fact that many authors agreed that unsteady effects should play a major role in the arm propulsion, the lack of reliable experimental data prevented the development of meaningful physical models. Lauder and Dabnichki [6] produced the first experiments that measured directly the torque on an instrumented robotic arm. The obtained results challenged the common perception of the force profile and were somewhat different to understand. In order to obtain a reliable model a stepwise approach was utilised that combined experimental and mathematical models.

### 2.1 Lift and drag properties of the human arm

The first step was to obtain the physical characteristics of the arm. This process involves direct measurement at different configurations and different flow speed. The results of this study are presented in [3]. Once this results were obtained, they showed that drag and lift properties are not a sinusoidal function of the body drag when perpendicular to the flow and that the elbow angle changes in non-linear manner the drag and lift coefficients. These improved data improved the reliability of the estimate but there was still big discrepancy (direct torque in Fig.1 below is the one of the robotic arm and WT torque is the windtunnel one). As it as evident that the discrepancy is in the initial phase of the stroke, the natural explanation is that in this phase the arm acceleration is highest. Hence the most likely cause is the added mass effect.

### 2.2 Added mass effect

An incident irrotational flow past a three-dimensional rigid body translates with velocity $\overline{U}$ as immersed into a volume with surface $S_\infty$. The harmonic potential is decomposed into the incident flow that prevails in absence of the body $\phi^\infty$ and the disturbance potential due to the body $\phi^D$

$$\phi = \phi^\infty + \phi^D \tag{1}$$

The boundary integral representation for the disturbance component $\phi^D$ at a point $\overline{x}_0$ is

$$\phi^D(\overline{x}_0) = -\int_B G(\overline{x}_0, \overline{x})\left[\overline{U} - \nabla\phi^\infty(\overline{x})\right]\cdot \overline{n}(\overline{x}) dS(\overline{x}) + \int_B \nabla G(\overline{x}_0, \overline{x})\cdot \overline{n}(\overline{x})\phi^D(\overline{x}) dS(\overline{x}) \tag{2}$$

where *B* denotes the body surface and $G(\overline{x}, \overline{x}_0)$ is the free-space Green's function of Laplace's equation. The integrals over the infinite boundary surface $S_\infty$ are infinitesimal and are not shown in the equation. Rearranging the equation (2) eliminating the single-layer potential it is obtained

$$\phi(\overline{x}_0) = \phi^\infty(\overline{x}) - \int_B \nabla G(\overline{x}_0, \overline{x})\cdot \overline{n}(\overline{x})\left[\overline{U}\cdot \overline{x} - \phi(\overline{x})\right] dS(\overline{x}) \tag{3}$$

The above equation is a representation for the disturbance potential in terms of a double layer potential alone. By considering the case of a flow due to a rigid body moving with linear velocity $\overline{U}$ and angular velocity $\overline{\Omega}$ about the point $\overline{x}_c$, the no-penetration condition on the surface of the body requires that

$$\nabla\phi(\overline{x})\cdot \overline{n}(\overline{x}) = \left[\overline{U} + \overline{\Omega}\times(\overline{x} - \overline{x}_c)\right]\cdot \overline{n}(\overline{x}) \tag{4}$$

Due to the linearity of the flow governing equations and the no-penetration boundary condition, the velocity potential can be expressed as a linear combination of the translation and angular velocity about a point $\overline{x}_c$, situated in the interior of the body, as

$$\phi(\overline{x}) = U_i(t)\ \Phi_i\left[\overline{x}, \overline{x}_c(t), \overline{e}(t)\right] + \Omega_i(t)\ \Phi_{i+3}\left[\overline{x}, \overline{x}_c(t), \overline{e}(t)\right] \tag{5}$$

$\Phi_i$ are six harmonic potentials corresponding to three translations and three of rotations. The vector $\overline{e}$ describes body's instantaneous orientation. The no-penetration boundary condition requires that

$$\nabla\Phi_i(\overline{x})\cdot \overline{n}(\overline{x}) = \begin{cases} n_i(\overline{x}) \ldots\ldots\ldots\ldots\ldots\ldots\ldots i = 1,2,3 \\ \left[(\overline{x} - \overline{x}_c)\times \overline{n}(\overline{x})\right]_{i-3} \ldots\ldots\ldots i = 4,5,6 \end{cases} \tag{6}$$

The kinetic energy for a flow generated by the motion of a rigid body is expressed as

$$K = -\rho\frac{1}{2}\overline{U}\cdot \int_B \phi(\overline{x})\overline{n}(\overline{x}) dS(\overline{x}) = -\rho\frac{1}{2}\overline{\Omega}\cdot \int_B \phi(\overline{x})(\overline{x} - \overline{x}_c)\times \overline{n}(\overline{x}) dS(\overline{x}) \tag{7}$$

The above expresses the instantaneous kinetic energy of a potential flow in terms of a boundary integral that is a function of the distribution of $\phi$ over the boundary and the normal component of the velocity. Introducing the six-dimensional vector

$$\overline{W} = \left(U_x, U_y, U_z, \Omega_x, \Omega_y, \Omega_z\right) \tag{8}$$

the compact quadratic form for the kinetic energy is defined as

$$K = \frac{1}{2}\rho V_B A_{ij} W_i W_j \tag{9}$$

where A is the six-by-six grand added matrix defined as $A_{ij} = -\frac{1}{V_B}\int_B \Phi_i N_j dS$ with N is a six-dimensional vector whose first and second entry blocks contain the vectors *n* and $(\bar{x} - \bar{x}_c) \times \bar{n}$ respectively.

$$\alpha_{ij} = -\frac{1}{V_B}\int_B \Phi_i n_j dS \tag{10}$$

and $$\beta_{ij} = -\frac{1}{V_B}\int_B \Phi_{i+3} n_j dS \tag{11}$$

comprise respectively the three-by-three blocks on the major diagonal of $A$. From the equation of the added mass matrix is evident that the value of *A* depends exclusively upon the instantaneous body shape and orientation, but is independent of the body's linear or angular velocity or acceleration. Physically, *A* measures the sensitivity of the fluid's kinetic energy to the translational and rotational velocities of the moving body and may thus be regarded as an influence matrix for the kinetic energy. The matrix *A* is symmetric, i.e. the kinetic energy of the fluid when the body undergoes a translation along axis *i* and rotation about *j* is identical to the one generated by the body translation along *j* and rotation about *j*, with the same magnitude of the linear and angular velocities and crucially the matrix is also positive definite.

Once the Added Mass matrix is obtained then the global hydrodynamic forces acting on the body could be obtained. In particular the drag force (along the horizontal direction) and the lift force acting along the vertical y-axis. A combination of both forces in the direction of body motion is the propulsive force. The computational simulation was conducted on a three dimensional model of human arm performing front crawl stroke. The arm surface mesh contained 1024 six-nodded triangular rigid spherical shell elements.

A single degree of freedom motion was analysed, as the experimental data available were obtained from a single rotation about the shoulder with variable speed. The kinematic variable was the angle of attack - the angle between plane of the arm (defined as the plane containing the shoulder, elbow and wrist) and the flow direction. The range of motion was $0^o$ - $130^o$ (slightly more than the normal stroke range) in increments of $10^o$. The computer simulation was conducted for different arm configurations in terms of elbow flexion. The analysed configurations shown below are for elbow angles of $180^o$, $160^o$. This approach allowed to both assessing the effect of the added mass and the suitability of the BEM for use in such problems. The BEM, as shown below, proved reliability in both efficiency and accuracy. The main advantage is the low cost of the computation over alternative methods which require discretising the whole of the solution domain, re-gridding the entire volume for any angle of attack and initial conditions.

### 2.3 Free surface effect

An interface between a gas and liquid is often referred to as free surface. The presence of a free or moving boundary introduces serious complications for any type of analysis. In theory the presence of the free surface should affect the force generation especially in the initial phase when the arm is close to the water. The free-surface requires the introduction of special methods to define their location, their movement and their influence on a flow. Conceptually the simplest means of defining and tracking a free-surface is to construct a Lagrangian grid that is embedded and moves with the fluid. In our study we used free-surface flow modeling method based on the fractional volume of fluid concept. The volume of fluid (VOF) method, used by Fluent@, relies on the fact that two or more fluids (or phases) are not interpenetrating. For each additional phase that must be added to the model, a variable is introduced: the volume fraction of the phase in the computational cell. In each control volume, the volume fractions of all phases sum to unity. The fields for all variables and properties are shared by the phases and represent volume-averaged values, as long as the volume fraction of each of the phases is known at each location. We will refrain of presenting the method as most commercial CFD codes are furnished wih it.

## 3 Results

The results presented in figure 1-4 below represent the evolution of the model from a steady fluid mechanics of a bluff body (the windtunnel torque) through the quasi-steady – bluff body lift and drag plus added mass effect and finally the effect of the free surface.

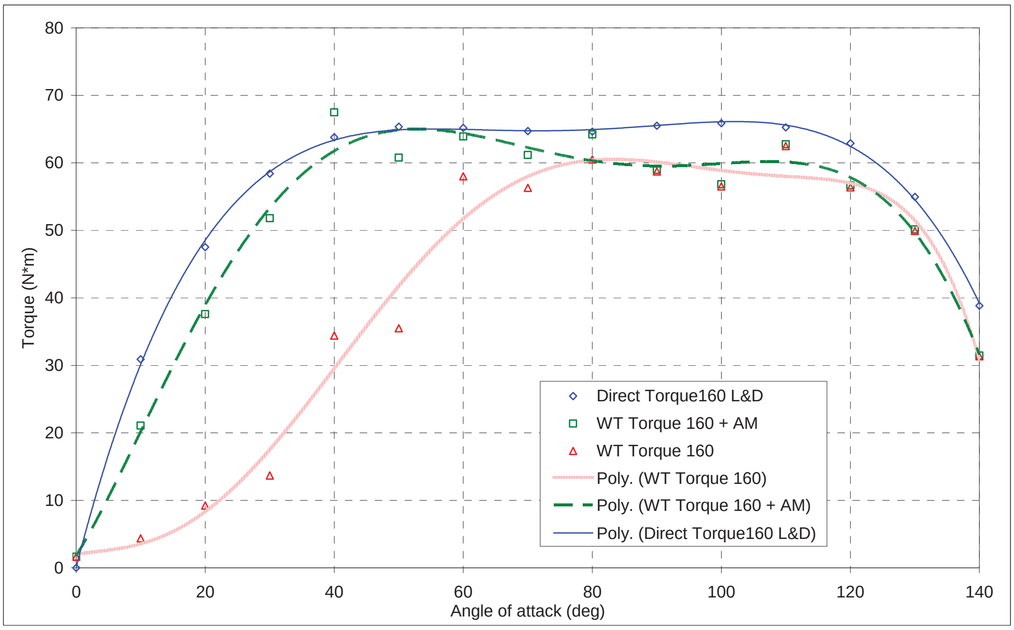


**Figure 1**. Torque comparison between wind tunnel experiment results (with and without added mass correction) and data obtained in a water tank on a model of arm. Elbow configuration $180^0$.

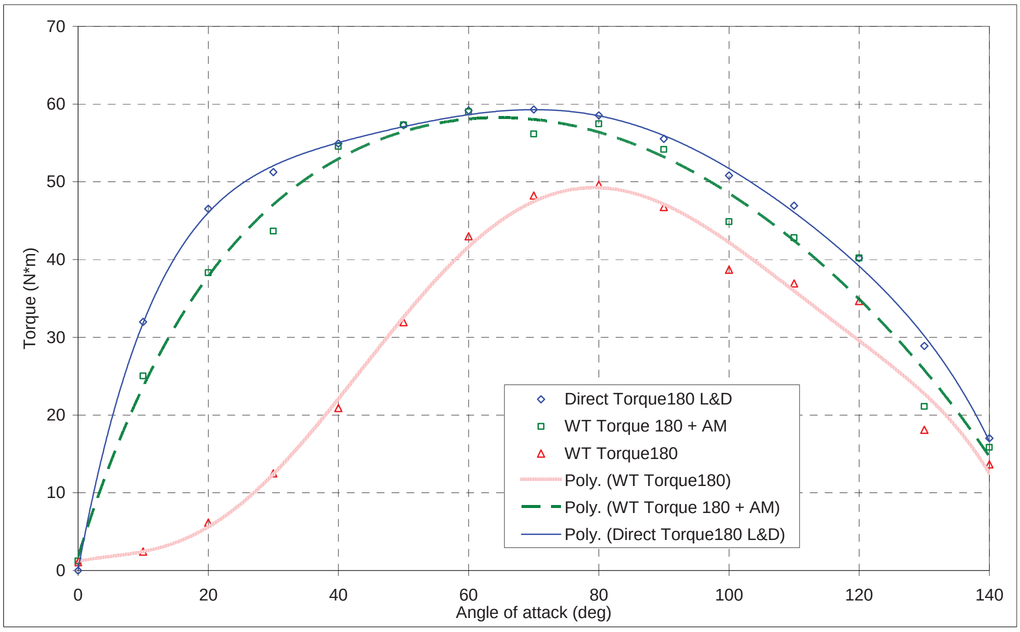


**Figure 2**. Torque comparison between wind tunnel experiment results (with and without added mass correction) and data obtained in a water tank on a model of arm. Elbow configuration $180^0$.

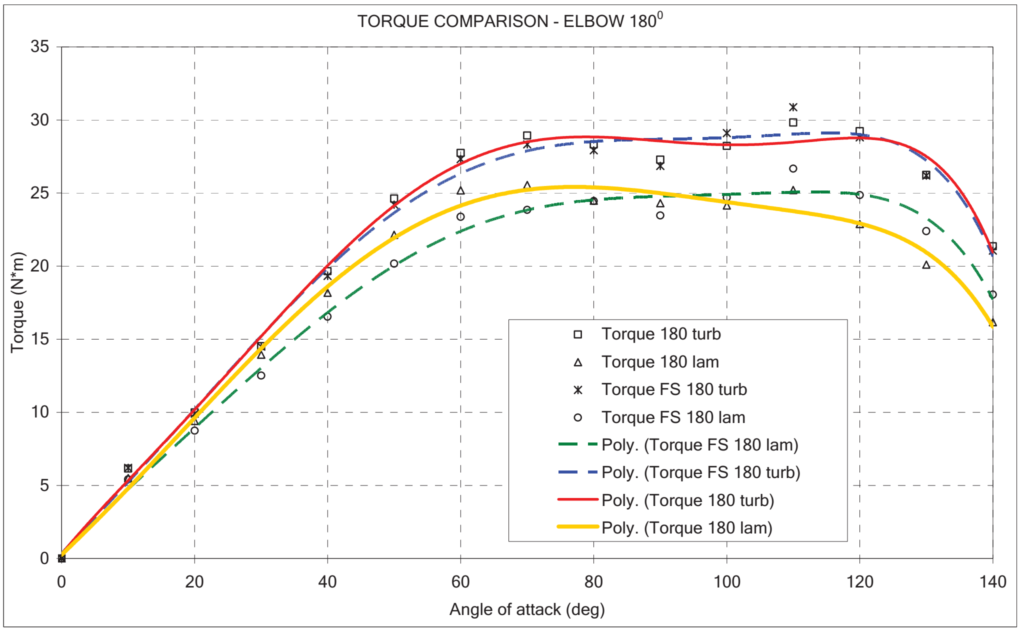


**Figure 3**. Torque comparison between laminar and turbulent flow in the presence and absence of free-surface (FS). Elbow configuration 180$^0$.

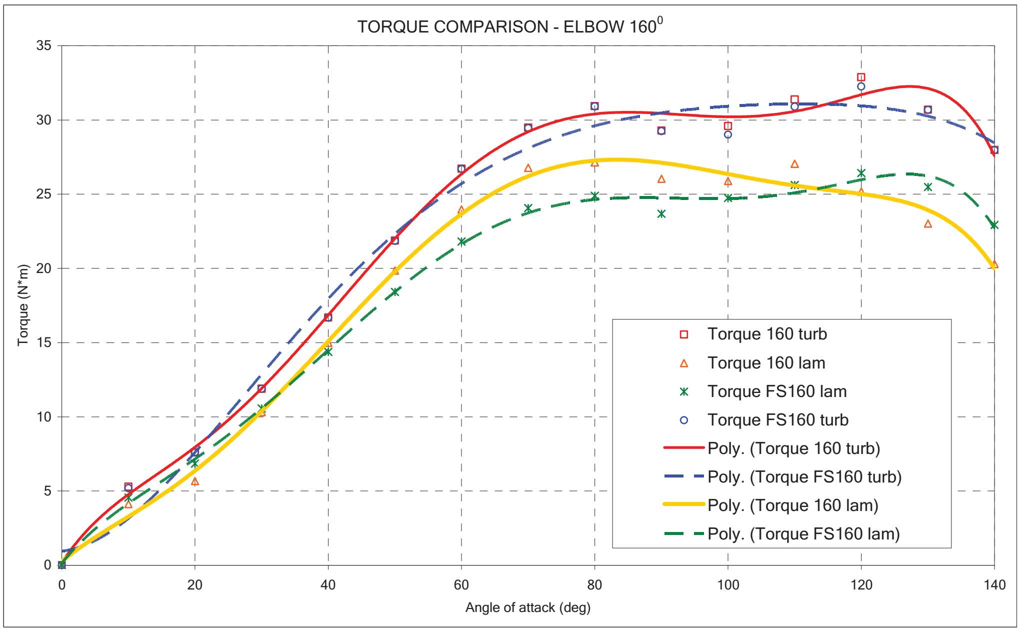


**Figure 4**. Torque comparison between laminar and turbulent flow in the presence and absence of free-surface (FS). Elbow configuration 160$^0$.

## 4 Discussion

The results presented above show clearly the relative importance o the different unsteady fluid flow factors in propulsion generation. It became clear that a quasi-steady approach provides a powerful tool for understanding of the mechanism of propulsive force. Furthermore, surprisingly the turbulence of the flow is of negligible importance. One should note that this statement applies for the underwater phase of the stroke. Although any authors [5,6,9] described the so called vortex shedding as an important phenomenon, the model did not consider it and we believe that the real phenomenon is attachment of flow to the arm rather than vortex generation. In the work we considered irrotational flow, i.e. no vortices and reached a good agreement. The vortex shedding effect that some studies report may be related to the cavitations caused by the arm entering the water. In any case the added mass effect could model the contribution of the vortices although they do not seem sufficiently important.

The free surface effect seems of minor importance as evident from figures 3 and 4. Furthermore, such modelling is rather arbitrary as physically meaningful inputs could neither be measured or derive theoretically. It seems strange that a simplified approach such as potential flow could be applied to at first glance a highly non-linear unsteady problem. However, the potential flow allows singularities that are powerful tool in modelling unsteady flow effects – such as added mass effect. In essence the use of BEM is a better option than the use of complex and computationally expensive Navier-Stokes solvers. Furthermore this approach is physically sound. The proposed model does not utilise numerical tricks such as artificial viscosity, small turbulence etc to achieve convergence and is mathematically proven unlike some favoured CFD approaches such as large eddy or direct numerical simulations.

## 5 Conclusion

A model for the arm propulsion was developed. In the process the relative contribution of different flow phenomena was assessed and understood. The agreement with specifically obtained experimental data was very good proving the physical soundness of the model as the mathematical one is clear as the model is based on the Laplace’s equation. It should be noted that the limit of the proposed model is that the motion frequency need to be relatively low and multi-segmental motion will not be modelled effectively. Hence modelling the propulsion generation of aquatic species poses further challenges. Current work is now devoted to fully dynamic model again within the potential flow assumptions which we found to be physically sound.

## 6 References

[1] Childress, S., Mechanics of Swimming and Flying, 1st Edition, Cambridge University Press (1981)

[2] Dabnichki P.: *Modelling, Computing and Sport,* Informatik Spektrum, 31 (2008), 316-323.

[3] Gardano, P. and Dabnichki, P., *On hydrodynamics of drag and lift of the human arm*, Journal of Biomechanics 39 (2006) pp 2767-2773

[4] Jane Wang, Z., *Vortex shedding and frequency selection in flapping flight*, Journal of Fluid Mechanics 410 (2000), pp 323-341

[5] Kazuo, M., Yamada, K., Takahiro, M., Jun, S. and Takeo, N., *Hand motion and the generation of propulsive force of crawl swimmers*, 12th annual congress of the ECCS, 11-14 July 2007, Jyvaskyla, Finland

[6] Lauder, M.A. and Dabnichki, P., *Estimating propulsive forces – sink or swim?*, Journal of Biomechanics 38 (2005), pp 1984-1990

[7] Michelson, R.C. and Naqvi, M.A., *Beyond biologically-inspired insect flight*, Low RE aerodynamics on aircraft including applications in emerging UAV technology RTO-AVT von Karman institute for Fluid Dynamics lecture Series, Nov. 24-28, 2003

[8] Ross, S.D., *Optimal flapping strokes for self-propulsion in a perfect fluid*, Proceedings of the 2006 American control conference, Minneapolis, Minnesota, USA, June 14-16, 2006

[9] Rouboa, A., Silva, A., Leal, L., Rocha, J., and Alves, F. 2006. The Effect of Swimmer’s Hand/Forearm Acceleration on Propulsive Forces Generated Using Computational Fluid Dynamics. *Journal of Biomechanics* 39, pp 1239-1248

[10] Rozhdestvensky, K.V. and Ryzhov, V.A., *Aerohydrodynamics of flapping-wing propulsors*, Progress in aerospace science 39 (2003), pp 585-633